Proceedings of the 2016 IEEE/SICE International Symposium on System Integration, Sapporo Convention Center, Sapporo, Japan, December 13-15, 2016

A 3D Printed Soft Gripper Integrated with Curvature Sensor for Studying Soft Grasping

Zhongkui Wang and Shinichi Hirai

***Abstract*— The grasping dynamics between a soft gripper and a deformable object has not been investigated so far. To this end, a 3D printed soft robot gripper with modular design was proposed in this paper. The gripper consists of a rigid base and three modular soft fingers. A snap-lock mechanism was designed on each finger for easy attach-detach to the base. All components were 3D printed using the Objet260 Connex system. The soft finger is air-driven and the idea is based on the principle of fluidic elastomer actuator. A curvature sensor was integrated inside each finger to measure the curvature during grasping. The fingers integrated with sensors were calibrated under different pneumatic pressure inputs. Relationship between pressure loading and bending angle, and relationship between bending angle and sensor output (voltage) were derived. Experiments with the gripper grasping and lifting a paper container filled with peanuts were conducted and results were presented and discussed.**

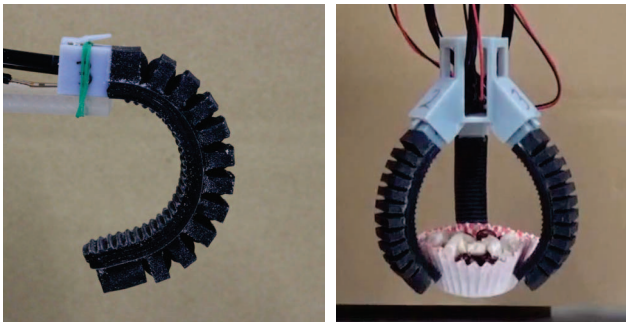

(a) (b)

Fig. 1. Soft finger (a) and soft gripper grasping and lifting a soft container filled with peanuts (b).

I. INTRODUCTION

Soft robotics is an emerging field and it differs from the traditional robotics not only because the robot itself includes soft deformable parts but also because the manipulating targets involves soft and deformable objects. Rigid hand or gripper handling rigid objects has always been an active field in robotics and many dexterous hands and grippers, such as the Shadow Dexterous Hand™ and the BarrettHand™, have been developed and studied. By equipping tactile sensors, such as the BioTac®, on these rigid hands or grippers, grasping and manipulating soft and deformable objects became possible [1]. Using soft hand or gripper to manipulate rigid objects has also been studied theoretically [2], [3] and practically [4], [5]. On the other hand, using soft robotic hand or gripper to grasp or manipulate soft and deformable objects has not been studied extensively.

In recent years, soft elastomer robot grippers have drawn great attention in many applications due to its characteristic of high compliance and resilience. Developments of soft gripper can date back to the 90s. Suzumori *et al.* first proposed a flexible microactuator driven by electro-pneumatic system and this small cylindrical actuator can realize pitch, yaw, and stretch motions [6]. A soft gripper integrating four such microactuators can perform several different grasping tasks even screw in a bolt. A recent review in [7] summarized the design, fabrication, and control of soft robots. It states that soft robots provide an opportunity to bridge the gap between machines and people. More specifically for soft fluidic elastomer robots, a review was written by Marchese *et al.* introducing the details of design and fabrication [8]. According to [8], soft fluidic elastomer robots can be divided into three types: ribbed, cylindrical, and pleated, based on the actuator morphology. The grippers proposed in this paper is based on the pleated type morphology. Similar idea and design were previously introduced in [8], [9], [10] and was extended in [4] by adding a bend sensor to measure the curvature of the actuator. In [10], the soft gripper was used to perform pick-and-place experiments with more than 70 randomly selected daily objects and the comparison with traditional rigid gripper was made. A recent application of such a gripper can be also found in [11] for biological sampling on deep reefs. Other examples can be also found in a starfish-like soft gripper [12] and an anthropopathic soft hand [13] for achieving dexterous grasping. These grippers successfully grasped some delicate objects, such as an egg in [12] or a disk and chopsticks in [13]. One downside of such a gripper is the relatively complex fabrication process which consists of several manual molding processes, assembling, and wax melting. Complex manual fabrication in turns enlarges the individual differences of the gripper and makes the generalization of quantitative analysis difficult.

In this work, we proposed a 3D printed soft gripper for studying soft grasping between a soft gripper and a deformable object, such as a paper container filled with peanuts (Fig. 1). In Section II, we introduce the design of the finger and the gripper, followed by the explanation of the fabrication process in Section III. Calibration of the finger integrated with curvature sensor was presented in Section IV, followed by the grasping experiments in Section V. The paper was concluded in Section VI with suggestions of future work.

*This work is supported by MEXT Kakenhi 26860404, JSPS, Japan

The authors are with the Soft Robotics Laboratory, Department of Robotics, Ritsumeikan University, 525-8577 Kusatsu, Japan. {wangzk at fc, hirai at se}.ritsumei.ac.jp

978-1-5090-3329-4/16/$31.00 ©2016 IEEE

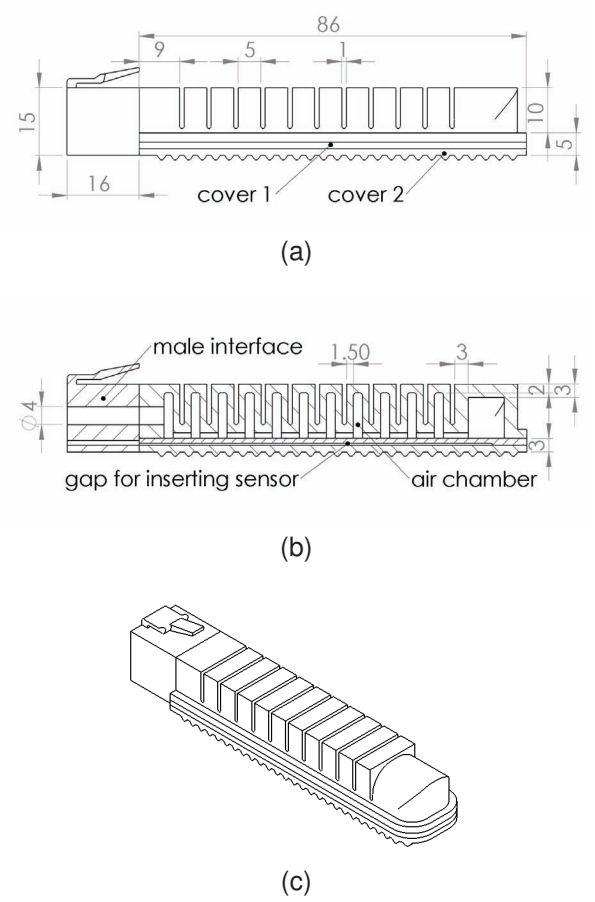

Fig. 2. The design drawings of a single finger in (a) the front view, (b) the section view, and (c) the isometric view.

II. Finger and Gripper Design

The single finger design is based on the idea of the pleated type morphology of the fluidic elastomer robot. As shown in Fig. 2, the soft finger is a combination of a male interface and twelve soft air chambers. The rigid male interface is designed for easy connection to the gripper base. Among the twelve air chambers, eleven chambers have a wall thickness of 1.5 mm and one larger chamber has a wall thickness of 3 mm. The thicker wall of the larger chamber makes the finger end stiffer than the rest of the finger to mimic the function of human nail. There are two covers under the chambers to seal the chambers from leaking. A groove (0.45 mm) was cut into the cover 1 to allow the insertion of the curvature sensor. Rippled structure was designed on the bottom surface of the cover 2 to increase the grasping stability and mimic the human fingerprint. The soft part of the finger has a length of 86 mm. A hole with a diameter of 4 mm was cut through the male interface to allow the insertion of the air hose.

To construct a three-fingered gripper, a base was designed with three female interfaces distributed circularly as shown in Fig. 3a. A snap-lock mechanism was designed on the male and female interfaces for easy attach-detach between the fingers and the base without using screws. A flange was designed on the top of the base for easy attach to a robot arm. By connecting three fingers to the base, we have an

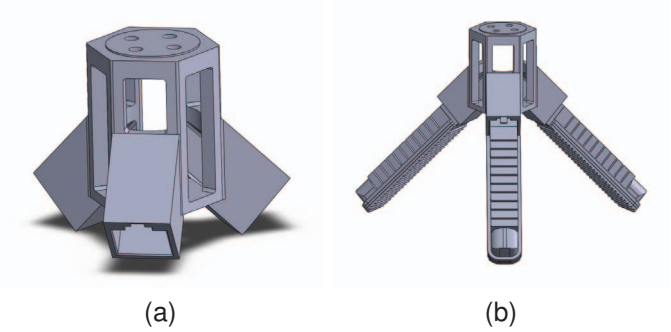

Fig. 3. The 3D model of the base (a) and the assembly of the soft gripper with three fingers (b).

assembled soft gripper as shown in Fig. 3b. The open space on the base body is designed to allow the air hose and the sensor wire cables passing through.

III. Fabrication of the Gripper

The grippers were printed using a state-of-the-art 3D printer (EDEN260V/Objet260Connex^{TM} system). This printer can print 14 digital materials simultaneously with different mechanical properties by mixing a soft rubber-like material (TangoBlack+) and a hard polypropylene-like material (VeroWhite). The 3D printer requires '.stl' file for printing as the same as most of normal 3D printer. For printing a single part consisting multiple materials, each region with single material should be designed separately and then assembled together as an assembly file. Detailed introduction of the printing principle using such a printer can be found in [14].

The soft finger was printed as three separate parts as shown in Figs. 4a, 4b, and 4c. The soft air chambers and the rigid

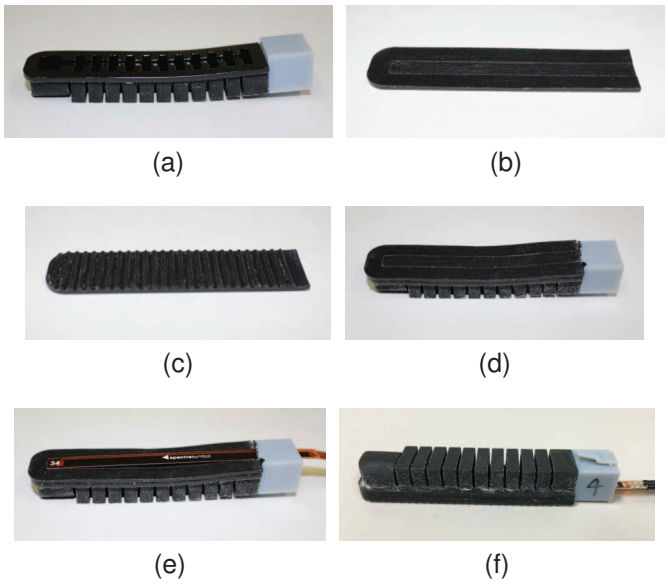

Fig. 4. The fabrication process of a single finger. 3D printed separate parts of (a) the chambers and the male interface, (b) the cover 1, and (c) the cover 2. Sub-figure (d) shows the chambers glued and sealed with the cover 1, (e) shows the finger after inserting the curvature sensor, and (f) shows the complete soft finger.

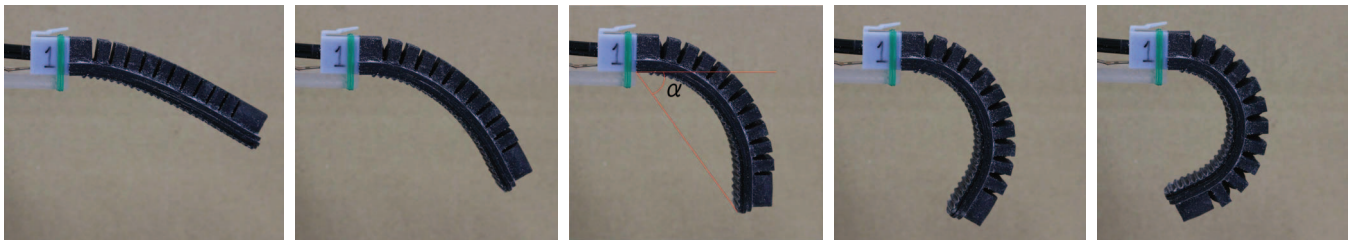

(a) P = 0 kPa (b) P = 10 kPa (c) P = 20 kPa (d) P = 30 kPa (e) P = 40 kPa

Fig. 5. Experimental snapshots of soft finger No. 1 under different air pressure loadings.

TABLE I
RELATIVE STANDARD DEVIATION (RSD) OF BENDING ANGLES UNDER DIFFERENT AIR PRESSURE LOADINGS

Pressure	Finger 1	Finger 2	Finger 3	Among fingers
P = 0 kPa	8.12%	6.36%	8.99%	3.27%
P = 10 kPa	4.28%	3.18%	5.13%	2.72%
P = 20 kPa	3.93%	1.44%	2.53%	1.58%
P = 30 kPa	1.89%	1.07%	1.85%	0.66%
P = 40 kPa	1.70%	0.93%	1.38%	0.47%

male interface were printed simultaneously using the soft material (TangoBlack+) and hard material (DM_8520_Grey40), respectively. The cover 1 and 2 were printed using the soft material and each has a thickness of 1.5 mm. After removing the support materials, the parts were washed with clean water and dried out at room temperature. The cover 1 was then glued on the air chambers (Fig. 4d) to seal them from leaking using a rubber targeted glue (ThreeBond 1521B). A curvature sensor (SPECTRASYMBOL-001, SWITCHSCIENCE) was inserted through the slot on the male interface and fitted in the groove on the cover 1, as shown in Fig. 4e. Finally by gluing the cover 2 on the cover 1, the soft finger was completed as shown in Fig. 4f.

IV. SINGLE FINGER CALIBRATION

Three soft fingers were fabricated and the single finger calibration was performed. An air compressor (JUN-AIR 3-4) and an electro-pneumatic regulator (SMC® ITV2030) were used to generate constant air pressures. Four different pressures were applied to each finger and the voltages generated on the curvature senors were recorded using an Arduino board. Photo snapshots (Fig. 5) were taken during experiments and bending angles α (Fig. 5c) were calculated for analysis. Three calibration trials for each finger were conducted and the calibration results were presented below.

A. Relationship of Air Pressure and Bending Angle

Figures 6a, 6b, and 6c show the relationship curves of applied air pressure and the bending angle for different experimental trials of each soft finger, respectively. Figure 6d show the differences among different soft fingers, in which average responses of three trials were plotted. Table I shows the relative standard deviation (RSD) of the bending angles under different pressure loadings. We found that the differences among different trials and different fingers are not significant and RSDs are less than 5% for most of the cases. We also found that the RSD decreases along the increase of the pressure loading. This tells us that the difference in finger structure during fabrication dominates the RSD in low pressure loadings and it becomes negligible in high pressure loadings. Results shown in Fig. 6 and Table I validated the bending repeatability of the soft finger. Once the finger structure and material was determined, the bending angle and the applied air pressure have an approximately linear relationship. By approximating the average response of three fingers, we derived the following equation to predict the bending angle under a certain air pressure while no grasping involved.

$$\theta = 1.588P + 25.34, \tag{1}$$

where P denotes the applied air pressure (kPa) and θ is the generated bending angle (°).

B. Relationship of Voltage and Bending Angle

Figures 7a, 7b, and 7c show the relationships between the bending angle and the voltage output from the curvature

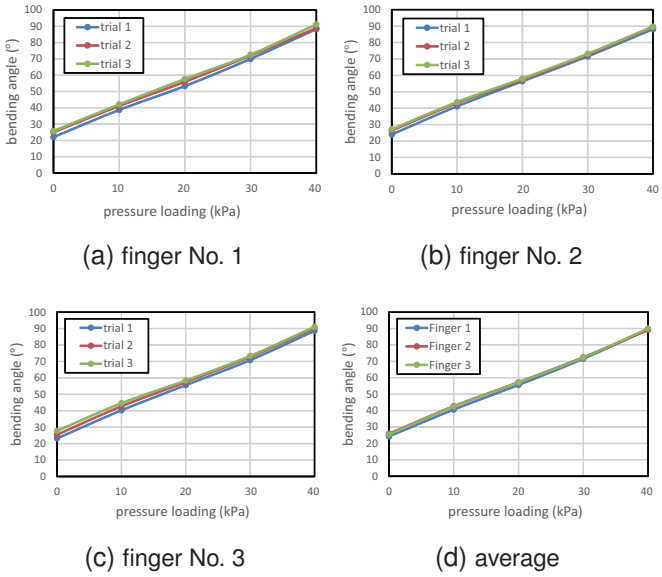

(a) finger No. 1 (b) finger No. 2

(c) finger No. 3 (d) average

Fig. 6. The relationships between the applied air pressure and the bending angle for different soft fingers in (a), (b), and (c). Sub-figure (d) shows the comparison between different fingers.

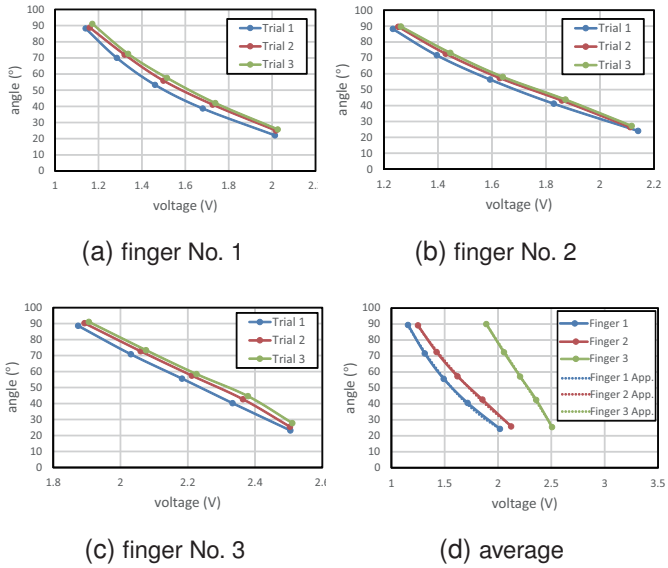

Fig. 7. The relationships between voltage output and bending angle for different soft fingers in (a), (b), and (c). Sub-figure (d) shows the comparison between different fingers.

TABLE II
RELATIVE STANDARD DEVIATION (RSD) OF VOLTAGE OUTPUTS UNDER DIFFERENT AIR PRESSURE LOADINGS

Pressure	Finger 1	Finger 2	Finger 3	Among fingers
P = 0 kPa	0.33%	0.73%	0.15%	11.59%
P = 10 kPa	1.79%	1.19%	0.99%	17.16%
P = 20 kPa	1.90%	1.52%	0.99%	21.51%
P = 30 kPa	2.03%	1.79%	1.11%	25.07%
P = 40 kPa	1.35%	1.22%	0.85%	27.91%

sensor for different experimental trials of each finger, respectively. Figure 7d shows the differences among different soft fingers, in which average responses of three trials were plotted. Table II listed the RSDs of the voltage outputs under different pressure loadings. We found that the differences among different trials for each finger are not significant and the RSDs are less than 3%, which validates the repeatability of one single finger integrated with curvature sensor. On the other hand, the differences among different fingers are quite significant and the RSDs are larger than 15% for most of the cases. This tells us that the characteristic of each curvature sensor is quite unique and we have to calibrate each finger separately. In addition, nonlinearities were found in the relationships between the bending angle and the voltage. By approximating the curve of each sensor using quadratic polynomial equation, we have the following equations to describe the relationship for each finger. The dotted lines in Fig. 7d show the approximation results.

$$\begin{aligned} \text{Finger 1}: &\quad \theta = 44.49V^2 - 215.85V + 279.03, \\ \text{Finger 2}: &\quad \theta = 24.09V^2 - 152.55V + 241.64, \\ \text{Finger 3}: &\quad \theta = -4.43V^2 - 84.04V + 264.40, \end{aligned} \tag{2}$$

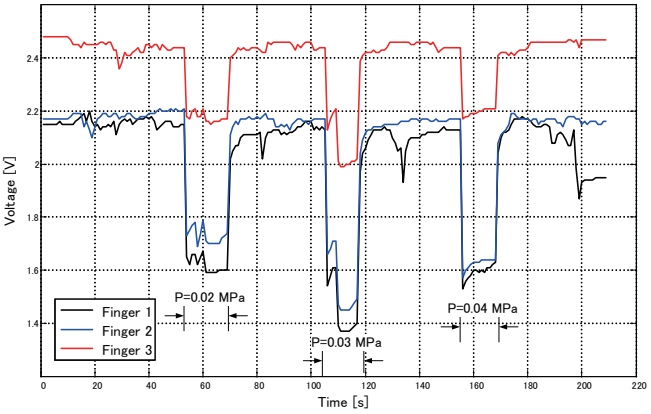

Fig. 8. Voltage outputs of the three curvature sensors during the grasping experiment.

where V denotes the voltage output (V) and θ is the generated bending angle (°).

V. GRASPING EXPERIMENTS

By connecting three fingers to the base and inserting air hose into each finger, we constructed the three-fingered soft gripper (Fig. 1b) for grasping experiment. Instant adhesive glue was used to seal the air hose insertion to prevent air leaking. The grasping target is a paper container filled with 50 g peanuts. 50 g is a standard weight of the dishes usually packed in a lunch box. The container is frustum-shaped with a size of ϕ80 mm (top) $\times\phi$48 mm (bottom) $\times$25 mm (height). Three constant air pressures: 20 kPa, 30 kPa, and 40 kPa, were applied on the gripper to grasp and lift the target. A ten seconds hanging without dropping is considered as a successful lift. The voltage outputs from three fingers recorded by an Arduino board were plotted in Fig. 8. We can clearly see the three grasping attempts indicated by the sudden drops of the voltage. Among the three attempts, the first two (P = 20 kPa and P = 30 kPa) were failed to lift the target up. The last attempt (P = 40 kPa) was a successful lift. Comparing with successful lift, failed lifts generated vibrations in voltage at the beginning of the lift. These vibrations were generated by the slippage between the fingers and the container surface. This surface vibration will be further investigated in the future.

The voltage output of the successful lift was highlighted in Fig. 9. During lifting, we found that the voltage outputs were gradually decreased from A to B because the fingers were stretched and bent less to support the target weight as the target was lifted. By substituting the voltages at moments A and B into Eq. 2, we can calculate the bending angles at these moments. The results were given in Table III together with the free bending angle under pressure 40 kPa, which can be calculated from Eq. 1. With an applied pressure of 40 kPa, the soft fingers were supposed to have a bending angle of 88.843°. However due to the contact with the paper container, the soft fingers were bent around 50° through 60°. The constrained angles (subtraction of the second column from the first column) can be related to

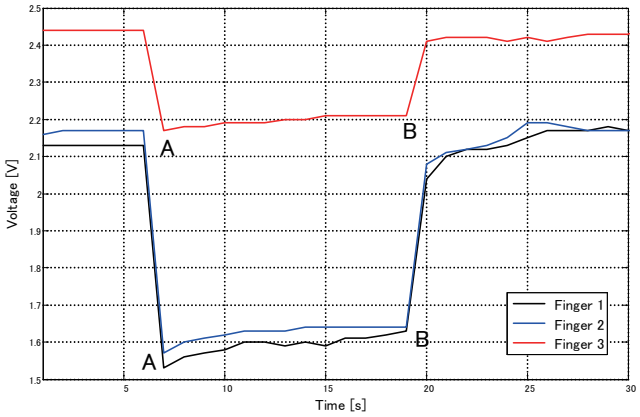

Fig. 9. Voltage outputs of the three curvature sensors during the successful lift.

TABLE III

BENDING ANGLES OF THE THREE FINGERS CALCULATED FROM THE GRASPING EXPERIMENT

Finger	P = 40 kPa	moment A	moment B
Finger 1	88.84°	52.93°	45.40°
Finger 2	88.84°	61.50°	56.24°
Finger 3	88.84°	61.18°	57.04°

the grasping force. This relationship can be calibrated with a series of constrained force tests. Bending angles at the moment A can be used to predict the approximate size of the target, but we need one more measure, such as the arc height of the finger curvature, or we need to develop a mathematical model to calculate the soft finger bending. The angle differences between moments A and B can be related with the weight of the grasping target. This again requires a mathematical model to describe the contact between the soft finger and the container surface. Apparently with only bending angle measured from the curvature sensor, it is hard to fully understand the target information and grasping dynamics. These issues will be tackled in our future works.

VI. CONCLUSIONS

To study soft grasping, a soft gripper integrated with curvature sensor was proposed in this paper. The gripper consists of three soft fingers and a rigid base. Snap-lock interfaces were designed on the finger and the base for easy assembly without using screws. All components were 3D printed with a state-of-the-art 3D printer, which is able to print multiple materials simultaneously including soft rubber-like materials. The soft finger design is based on the idea of the pleated type morphology of the fluidic elastomer robot. A commercial curvature sensor was integrated inside the soft finger to measure the bending angles during grasping. Single finger calibration was performed and we found that the soft finger has a good repeatability of bending angles under varying air pressures not only among different trials but also among different soft fingers. For the relationship between the voltage output and the bending angle, good repeatability was found among different trials of a single finger, but significant differences (RSD $>$ 15% for most cases) were found among different fingers and this suggested us to calibrate each finger individually before actual use. Relationship between applied air pressure and the bending angle, and the relationship between the bending angle and the voltage output were derived by approximating the corresponding experimental data. Experimental trial of grasping a paper container filled with peanuts was conducted with the soft gripper. We found that failed lifts generated vibrations at the beginning of the lift due to the slippage. Successful lift yielded gradual decrease of the bending angle due to the finger stretch caused by the target weight. The target size and weight can be related with the bending angle and the angle changes, but more information was required to clearly understand these relationships and these will be investigated in the future. A mathematical model for analyzing the curvature and the dynamics of the soft finger will be developed as well in our future work.

REFERENCES

[1] K. Sivakumar, C. H. Priyanka, "Grasping objects using Shadow dexterous hand with tactile feedback," International Journal of Innovative Research in Science, Engineering and Technology, Vol. 4, No. 5, May 2015, pp. 3108-3116.

[2] T. Inoue, S. Hirai, "Elastic model of deformable fingertip for soft-fingered manipulation," IEEE Transactions on Robotics, Vol. 22, No. 6, 2006, pp. 1273-1279.

[3] Y. Yamazaki, T. Inoue, S. Hirai, "Two-phased controller for a pair of 2-DOF soft fingertips based on the qualitative relationship between joint angles and object location," in Proc. 2010 IEEE International Conference on Robotics and Automation (ICRA), Anchorage, 2010, pp. 4294-4301.

[4] B. S. Homberg, R. K. Katzschmann, M. R. Dogar, D. Rus, "Haptic identification of objects using a modular soft robotic gripper," in Proc. 2015 IEEE/RSJ International Conference on Intelligent Robots and Systems (IROS), Hamburg, 2015, pp. 1698-1705.

[5] I. M. Bullock, C. Guertler, A. M. Dollar, "Patterned compliance in robotic finger pads for versatile surface usage in dexterous manipulation," in Proc. 2015 IEEE International Conference on Robotics and Automation (ICRA), Seattle, 2015, pp. 2574-2579.

[6] K. Suzumori, S. Iikura, H. Tanaka, "Development of flexible microactuator and its applications to robotic mechanisms," in Proc. 1991 IEEE International Conference on Robotics and Automation (ICRA), Sacramento, 1991, pp. 1622-1627.

[7] D. Rus, M. T. Tolley, "Design, fabrication and control of soft robots," Nature 521, 2015, pp. 467-475.

[8] A. D. Marchese, R. K. Katzschmann, D. Rus, "A recipe for soft fluidic elastomer robots," Soft Robotics, Vol. 2, No. 1, 2015, pp. 7-25.

[9] C. D. Onal, D. Rus, "A modular approach to soft robots," in Proc. the Fourth IEEE RAS/EMBS International Conference on Biomedical Robotics and Biomechatronics, Roma, 2012, pp. 1038-1045.

[10] R. K. Katzschmann, A. D. Marchese, D. Rus, "Autonomous object manipulation using a soft planar grasping manipulator," Soft Robotics, Vol. 2, No. 4, 2015, pp. 155-164.

[11] K. C. Galloway, K. P. Becker, B. Phillips, J. Kirby, S. Licht, D. Tchernov, R. J. Wood, and D. F. Gruber, "Soft robotic grippers for biological sampling on deep reefs," Soft Robotics, Vol. 3, No. 1, 2016, pp. 23-33.

[12] F. Ilievski, A. D. Mazzeo, R. F. Shepherd, X. Chen, G. M. Whitesides, "Soft robotics for chemists," Chemical Robotics, Angew. Chem. Vol. 50, No. 8, 2011, pp. 1890-1895.

[13] R. Deimel, O. Brock, "A novel type of compliant and underactuated robotic hand for dexterous grasping," The International Journal of Robotics Research, Vol. 35, No. 1, 2015, pp. 1-25.

[14] R. MacCurdy, R. Katzschmann, Y. kim, and D. Rus, "Printable hydraulics: a method for fabricating robots by 3D co-printing solids and liquids," in Proc. 2016 IEEE International Conference on Robotics and Automation, Stockholm, 2016, pp. 3878-3885.